UNSTABLE GALAXY MODELS

ZHIYU WANG, YAN GUO, ZHIWU LIN, AND PINGWEN ZHANG

Abstract. The dynamics of collisionless galaxy can be described by the Vlasov-Poisson system. By the Jean's theorem, all the spherically symmetric steady galaxy models are given by a distribution of $\Phi(E, L)$, where E is the particle energy and L the angular momentum. In a celebrated Doremus-Feix-Baumann Theorem [7], the galaxy model $\Phi(E, L)$ is stable if the distribution Φ is monotonically decreasing with respect to the particle energy E. On the other hand, the stability of $\Phi(E, L)$ remains largely open otherwise. Based on a recent abstract instability criterion of Guo-Lin [11], we constuct examples of unstable galaxy models of $f(E, L)$ and $f(E)$ in which f fails to be monotone in E.

1. Introduction

A galaxy is an ensemble of billions of stars, which interact by the gravitational field they create collectively. For galaxies, the collisional relaxation time is much longer than the age of the universe ([6]). The collisions can therefore be ignored and the galactic dynamics is well described by the Vlasov - Poisson system (collisionless Boltzmann equation)

$$\partial_t f + v \cdot \nabla_x f - \nabla_x U_f \cdot \nabla_v f = 0, \qquad \Delta U_f = 4\pi \int_{\mathbf{R}^3} f(t, x, v) dv, \tag{1}$$

where $(x, v) \in \mathbb{R}^3 \times \mathbb{R}^3$, $f(t, x, v)$ is the distribution function and $U_f(t, x)$ is its self-consistent gravitational potential. The Vlasov-Poisson system can also be used to describe the dynamics of globular clusters over their period of orbital revolutions ([9]). One of the central questions in such galactic problems, which has attracted considerable attention in the astrophysics literature, of [5], [6], [9], [16] and the references there, is to determine *dynamical stability* of steady galaxy models. Stability study can be used to test a proposed configuration as a model for a real stellar system. On the other hand, instabilities of steady galaxy models can be used to explain some of the striking irregularities of galaxies, such as spiral arms as arising from the instability of an initially featureless galaxy disk ([5]), ([17]).

In this article, we consider stability of spherical galaxies, which are the simplest elliptical galaxy models. Though most elliptical galaxies are known to be non-spherical, the study of instability and dynamical evolution of spherical galaxies could be useful to understand more complicated and practical galaxy models. By Jeans's Theorem, a steady spherical galaxy is of the form $f(x, v) \equiv \mu(E, L)$, where the particle energy and total momentum are $E = \frac{1}{2}|v|^2 + U(x)$, $L = |x \times v|$, and $U_\mu(x) = U(|x|)$ satisfies the self-consistent nonlinear Poisson equation

$$\Delta U = 4\pi \int_{\mathbf{R}^3} \mu(E, L) dv$$

The isotropic models take the form $f(x, v) \equiv \mu(E)$. The case when $\mu'(E) < 0$ (on the support of $\mu(E)$) has been widely studied and these models are known to be

stable ([1], [2], [7], [2], [8], [19], [14], [18], [13]). To understand such a stability, we expand the well-known Casimir-Energy functional (as a Liapunov functional)

$$\mathcal{H} \equiv \int\int Q(f) + \frac{1}{2}\int\int |v|^2 f - \frac{1}{8\pi}\int |\nabla_x U|^2 \tag{2}$$

which is conserved for all time with

$$Q'(\mu(E)) \equiv -E \tag{3}$$

(this is possible only if $\mu' < 0$!). Upon using Taylor expansion around a steady galaxy model of $[f(E,L),U]$, the first order variation vanishes due to the choice of (3), and the second order variation takes the form of

$$\mathcal{H}''_f[g,g] \equiv \frac{1}{2}\int\int_{f>0} \frac{g^2}{-f'(E)} - \frac{1}{8\pi}\int |\nabla_x U_g|^2. \tag{4}$$

The remarkable feature for stability lies in the fact that $\mathcal{H}''_\mu[g,g] > 0$ if $\mu' < 0$ ([1], [2], [7], [14]). This crucial observation leads to the conclusion that galaxy models with monotonically decreasing energy $\mu' < 0$ are linearly stable. On the other hand, for the case μ is *not* monotone in E, (3) breaks down, and $\mathcal{H}''_\mu$ is not well-defined, which indicates possible formation of instability. It is important to note that a negative direction of the quadratic form $\mathcal{H}''_f[g,g] < 0$ does *not* imply instability. In [12], an oscillatory instability was found for certain generalized polytropes $f(E,L) = f_0 L^{-2m}(E_0 - E)^{n-\frac{3}{2}}$ with $n < \frac{3}{2}, m < 0$, by using N-body code. This instability was later reanalyzed by more sophisticated N-body code in [3]. Despite progresses made over the years (e.g., [3], [10], [16], [17]), *no* explicit example of isotropic galaxy model $\mu(E)$ are known to be unstable.

The difficulty of finding instability lies in the complexity of the linearized Vlasov-Poisson system around a spatially non-homogeneous $\mu(E,L)$:

$$\partial_t g + v\cdot\nabla_x g - \nabla_x U_g\cdot\nabla_v\mu - \nabla_x U\cdot\nabla_v g = 0, \quad \Delta U_g = 4\pi\int_{\mathbf{R}^3} g(x,v)dv \tag{5}$$

for which the construction for dispersion relation for a growing mode is mathematically very challenging. In a recent paper ([11]), a sufficient condition was derived rigorously as follows:

Theorem 1. *Let $[f(E,L),U]$ be a steady galaxy model. Assume that $f(E,L)$ has a compact support in x and v, and μ' is bounded. Define auxiliary quadratic form for a spherically symmetric function $\phi(|x|)$ as*

$$[A_0\phi,\phi] \equiv \int_{\mathbf{R}^3} |\nabla\phi|^2 dx + 32\pi^3\int f'(E,L)\int_{r_1(E,L)}^{r_2(E,L)} \left(\phi-\bar{\phi}\right)^2 \frac{2LdrdEdL}{\sqrt{2(E-U(r)-L^2/2r^2)}}, \tag{6}$$

where $r_1(E,L)$ and $r_2(E,L)$ are two distinct roots to the equation

$$E - U(r) - L^2/2r^2 = 0 \tag{7}$$

and the average $\bar{\phi}$ is defined as

$$\bar{\phi}(E,L) = \frac{\int_{r_1(E,L)}^{r_2(E,L)} \frac{\phi(r)dr}{\sqrt{2(E-U_0(r)-L^2/2r^2)}}}{\int_{r_1(E,L)}^{r_2(E,L)} \frac{dr}{\sqrt{2(E-U_0(r)-L^2/2r^2)}}}.$$

If there exists $\phi(|x|)$ such that $[A_0\phi,\phi] < 0$, then there exists an exponentially growing mode to the linearized Vlasov-Poisson system (5).

The quadratic form $[A_0\phi, \phi]$ in the above instability criterion involves delicate integrals along particle paths. The purpose of the current paper is to use numerical computations to construct two explicit examples of galaxy models for which a test function ϕ satisfying $[A_0\phi, \phi] < 0$ exists. This ensures their radial instability by Guo-Lin's Theorem 1. The first example is an anisotropic model with radial instability. There are two differences to the oscillatory instability found in [12] and [3]: here the distribution function is non-singular and the instability is non-oscillatory. The second example is a non-singular isotropic model with radial instability. To our knowledge, this provides the first example of unstable isotropic model.

Even though the galaxy models studied here are not actual ones observed, our results demonstrates how to apply Guo-Lin's Theorem 1 to detect possible instability for a given galaxy model. It is our hope to foster interactions between mathematical and astronomical communities and to advance the study of instability of real galaxy models.

2. Examples of Unstable galaxy models

Example 1. **Unstable Galaxy Model Depending on E and L.** We define the distribution function $f_0(E, L) = \mu(E)L^4$ where

$$\mu(E) = \begin{cases} 0 & E < 4 \\ 2.25(E-4)^2 & 4 \le E \le 4.4 \\ (5-E)^2 & 4.4 \le E \le 5 \\ 0 & E > 5 \end{cases} \tag{8}$$

The graph of $\mu(E)$ is showed in Figure 1 below. Choosing $U(0) = 3$, we numerically

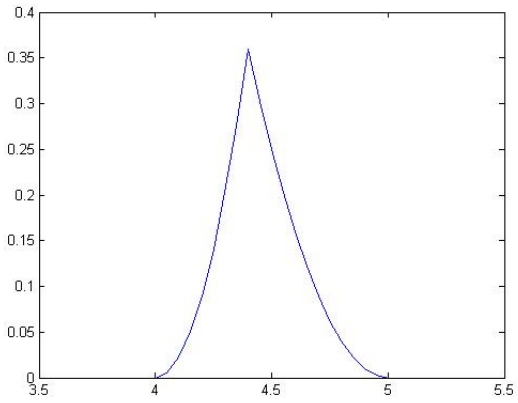

Figure 1. $\mu(E)$

calculate $U(r)$, and the graph of $U(r)$ is showed in Figure 2. By choosing the test function $\phi = e^{-r}$, then numerical computation below shows

$$[A_0\phi, \phi] < \pi - 45 < 0,$$

and hence f_0 is unstable by Theorem 1.

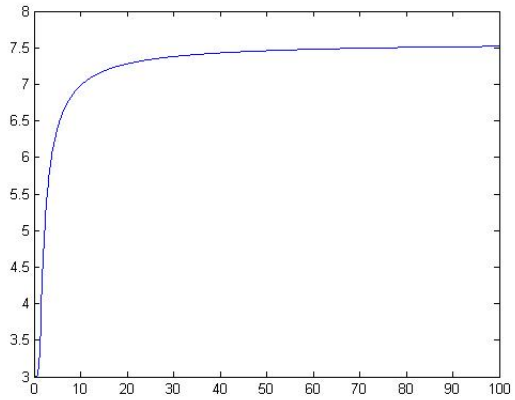

FIGURE 2. $U(r)$

Example 2. **Unstable Galaxy Model Depending Only on** E. Let $f_0(E) = \mu(E)$, where

$$\mu(E) = \begin{cases} 0 & E < a \\ C_1 t_1^k (E-a)^k & a \le E \le E_1 \\ C_1 (E_0 - E)^k & E_1 \le E \le E_0 \\ 0 & E > E_0 \end{cases} \tag{9}$$

We choose

$$C_1 = 2,\ E_0 = 5.1, a = 1.9,\ k = 2.01,\ t_1 = 1.5.$$

Choose $U_0 = -15.1$, the graphs of $\mu(E)$ and U are shown in Figures 3 and 4. We

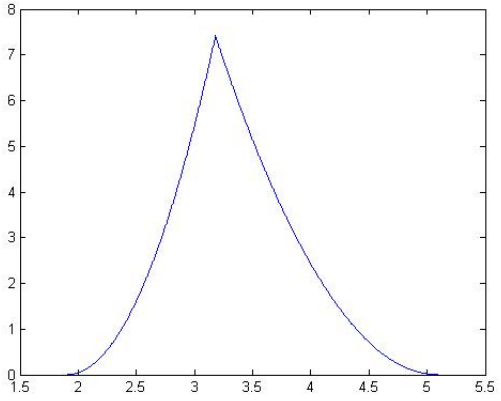

FIGURE 3. $\mu(E)$

choose the test function

$$\phi = v_1 e^{-r} + v_2 e^{-\frac{1}{2}r} + v_3 e^{-\frac{1}{3}r} + v_4 e^{-2r} + v_5 e^{-3r} + v_6 e^{-4r} + v_7 e^{-5r},$$

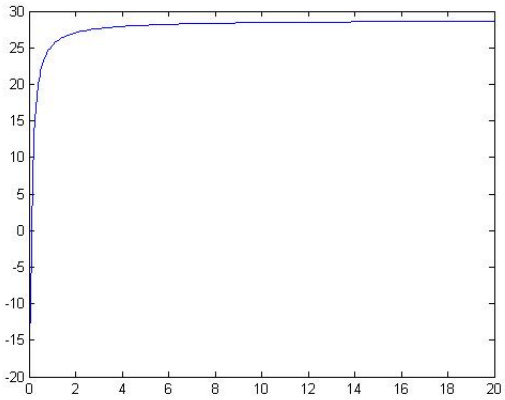

FIGURE 4. $U(r)$

with $v_1, v_2, ...v_7$ given by (16). Then $[A_0\phi, \phi] = -24.016 < 0$, and instability of the profile (9) follows from Theorem 1.

3. Numerical implementation

3.1. **Numerical computation for Example 1.** By the results in [20], for a steady state with $f_0(E, L) = \mu(E) L^{2l}$ of Vlasov-Poisson system, the steady potential $U(r)$ satisfies the equation

$$U'(r) = \frac{2^{l+7/2}\pi^2 c_{l,-1/2}}{r^2} \int_0^r s^{2l+2} g_{l+1/2}(U(s))ds, \quad r > 0 \tag{10}$$

with $g_m(u) = \int_u^\infty \mu(E)(E-u)^m dE, \quad u \in (-\infty, \infty), \quad$ and

$$c_{a,b} = \int_0^1 s^a (1-s)^b ds = \frac{\Gamma(a+1)\Gamma(b+1)}{\Gamma(a+b+2)}, \quad a > -1, b > -1,$$

where Γ denotes the gamma function. The boundary condition is $\lim_{r\to\infty} U(r) = 0$.

The computation of finding ϕ with $[A_0\phi, \phi] < 0$ is carried out in the following steps.

Step 1. Computation of potential U. For Example 1, $f_0(E, L) = \mu(E) L^4$ where $\mu(E)$ is given by (8), so $l = 2$ and

$$g_{l+1/2}(u) = \int_u^{4.4} 2.25(E-4)^2(E-u)^{2.5} dE + \int_{4.4}^5 (5-E)^2(E-u)^{2.5} dE.$$

Letting $M = 2^{l+7/2}\pi^2 c_{l,-1/2}$, we obtain from (10)

$$r^2 U''(r) + 2rU(r) = Mr^{2l+2} g_{l+1/2}(U(r)),$$

which is equivalent to

$$U''(r) = -\frac{2}{r}U'(r) + Mr^{2l} g_{l+1/2}(U(r)).$$

TABLE 1. L_{max} for different E

E	L_{max}
3.2	0.452787235493472
3.4	0.731586885359610
3.6	0.969996239842229
3.8	1.186531828839693
4.0	1.388987957485868
4.2	1.581703995145215
4.4	1.767449993848502
4.6	1.948250754546466
4.8	2.125722162034805
5.0	2.301341325775183

We use the boundary conditions $U'(0) = 0$ and $U(0) = 3$. Let $u_1(r) = U(r), u_2(r) = u_1'(r)$, we transform the above equation to the following system

$$\begin{cases} u_1'(r) = u_2 \\ u_2'(r) = -\frac{2}{r}u_2 + Mr^{2l}g_{l+1/2}(u_1) \end{cases} \tag{11}$$

with $u_1(r) = 3$ and $u_2(0) = 0$. We remark that we can subtract the finite limit of U at infinity from U and redefine E_0 accordingly. We apply Runge-Kutta method to solve equations (11), as follows

$$\begin{cases} \boldsymbol{y}_{n+1} = \boldsymbol{y}_n + \dfrac{h}{6}(\boldsymbol{K}_1 + 2\boldsymbol{K}_2 + 2\boldsymbol{K}_3 + \boldsymbol{K}_4) \\ \boldsymbol{K}_1 = \boldsymbol{f}(x_n, \boldsymbol{y}_n) \\ \boldsymbol{K}_2 = \boldsymbol{f}(x_n + \frac{h}{2}, \boldsymbol{y}_n + \frac{h}{2}\boldsymbol{K}_1) \\ \boldsymbol{K}_3 = \boldsymbol{f}(x_n + \frac{h}{2}, \boldsymbol{y}_n + \frac{h}{2}\boldsymbol{K}_2) \\ \boldsymbol{K}_4 = \boldsymbol{f}(x_n + h, \boldsymbol{y}_n + h\boldsymbol{K}_2). \end{cases}$$

First let $h = 0.1$ to get the values of U and U' at points $x_n = nh$, then we use piecewise cubic Hermite interpolation to get an approximation of $U(r)$.

Step 2. Computation of roots of the equation

$$E - U(r) - L^2/2r^2 = 0. \tag{12}$$

For fixed E, this equation has two solutions $r_1 < r_2$ when $L < L_{\max}$, one solution r^* when $L = L_{\max}$ and no solution when $L > L_{\max}$. Here, $L_{max}(E) = \sqrt{r^{*3}U'(r^*)}$ and $r^*(E)$ satisfies the equation

$$E - U(r) - \frac{r}{2}U'(r) = 0, \tag{13}$$

which comes from the combination of the equations $-U'(r) + L^2/r^3 = 0$ and (12). We employ Newton method to find the unique root r^* of (13) by the Newton iteration

$$r_{n+1} = r_n - \frac{E - U(r) - \frac{r}{2}U'(r)}{-\frac{3}{2}U'(r) - \frac{r}{2}U''(r)}$$

Chose an initial point $r_0 = 1$, we get r^*(with the stopping criterion $|r_n - r_{n+1}| < 10^{-10}$). Table 1 and Figure 5 show the relation of L_{max} to E.

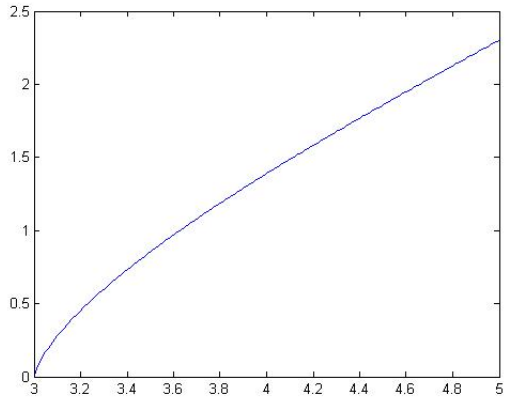

FIGURE 5. relationship of L_{max} and E

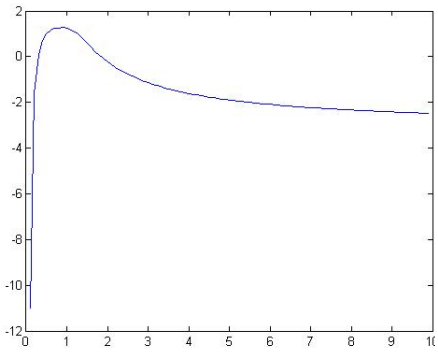

FIGURE 6. E=4.5,L=0.5

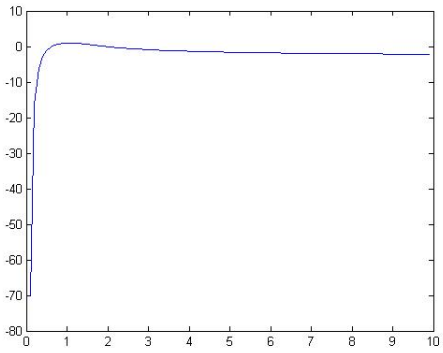

FIGURE 7. E=4.8,L=1.2

For $L < L_{max}$, we apply Newton's iteration

$$r_{n+1} = r_n - \frac{E - U(r) - L^2/2r^2}{-U'(r) + L^2/r^3}$$

to solve (12) with the choice of initial value

$$r_{1,0} = \begin{cases} 0.1 & \text{when} \quad L > 0.05, \\ 0.001 & \text{when} \quad L \leq 0.05 \end{cases}, \qquad r_{2,0} = 2,$$

and the stopping criterion $|r_n - r_{n+1}| < 10^{-10}$. We show two graphs of $E - U(r) - L^2/2r^2$ in Figures 6, and 7 and the computation results are

$$r_1 = 0.288701795314679, \ r_2 = 1.843722113067511 \quad \text{for Figure 6}$$

$$r_1 = 0.634700793130700, \ r_2 = 1.938943620330099 \quad \text{for Figure 7}$$

Figures 8 and 9 show how r_1 and r_2 ($r_1 < r_2$) change with respect to L, when E is given. (Note that the equation (12) has a unique root r^* when $L = L_{\max}$, thus when L approaches L_{max}, the distance $r_2 - r_1$tends to zero.)

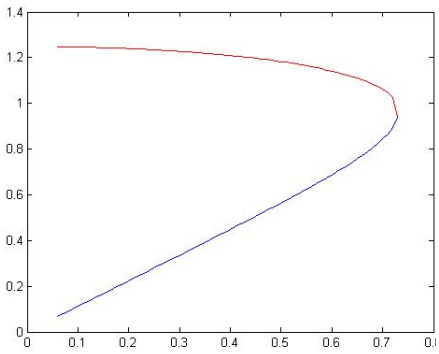

FIGURE 8. E=3.4, how r_1, r_2 change with L

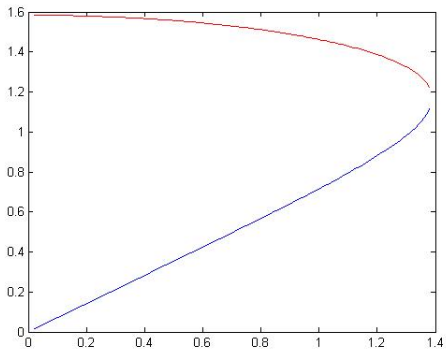

FIGURE 9. E=4, how r_1, r_2 change with L

TABLE 2. the value of $\mathcal{I}(E, L)$ for given E and L

(E, L)	$intergrand(E, L)$
(4.1,0.6)	0.002530474111772
(4.3,1)	0.053619816035575
(4.5,1.2)	-0.086444987713539
(4.7,1.3)	-0.086591041429108
(4.9,1.7)	-0.066267498867856

Step 3. Computing $A(\phi, \phi)$ in (6). Denote the integrand

$$\mathcal{I}(E, L) = f_0'(E, L) \int_{r1(E,L)}^{r2(E,L)} (\phi - \overline{\phi})^2 \frac{2Ldr}{\sqrt{2(E - U_0(r) - L^2/2r^2)}}.$$

Choose $\phi = e^{-r}$, Table 2 shows some of the values of $\mathcal{I}(E, L)$.

For given E, the integration interval of $\mathcal{I}(E, L)$ in (6) is $[0, L_{max}]$ for L. When $L = 0$ and $L = L_{max}$, (7) has only one solution instead of two. To avoid this problem, we integrate $\mathcal{I}(E, L)$ for L in the truncated interval $[a_1, L_{max} - a_2]$, where $a_1, a_2 > 0$. Choose $a_2 = 10^{-5}$, and compare the value of $\int_{a_1}^{L_{max}-a_2} \mathcal{I}(E, L)dL$ when $a_1 = 0.01$ and $a_1 = 0.001$ in Table 3. We see that the error is approximately 10^{-7}.

TABLE 3. Value of $\int_{a_1}^{L_{max}-a_2} \mathcal{I}(E, L)dL$ for $a_1 = 0.01$ and $a_1 = 0.001$

	$a_1 = 0.01$	$a_1 = 0.001$
$intergrandE(4.3)$	0.057831884696931	0.057831864357174
$intergrandE(4.5)$	-0.084810940209437	-0.084810952811088
$intergrandE(4.7)$	-0.095869703408813	-0.095869701098749
$intergrandE(4.9)$	-0.058302133990229	-0.058302146458761

Step 4. Error Estimate. Next we give a theoretical estimate for the error introduced by the truncation. Let $A(E) = \int_0^{r(E)} \frac{dr}{\sqrt{2(E-U(r))}}$, where $r(E)$ is the unique

solution of $E - U(r) = 0$. For $\phi(r) = e^{-r}$, the error term for L on $[0, a_1]$ is

$$\left| 32\pi^3 \int_4^5 \int_0^{a_1} \mu'(E)\, L^4 \int_{r_1(E,L)}^{r_2(E,L)} (\phi - \overline{\phi})^2 \frac{2L dr dL dE}{\sqrt{2(E - U(r) - L^2/2r^2)}} \right| \tag{14}$$
$$\leq \frac{64}{6}\pi^3 \int_4^5 |\mu'(E)| \max\left\{A(E), T(E, a_1)\right\} dE\ a_1^6.$$

In the above, we use the estimate

$$T(E,L) = \int_{r_1(E,L)}^{r_2(E,L)} \frac{dr}{\sqrt{2(E - U_0 - L^2/2r^2)}} \leq \max\{A(E), T(E, a_1)\}$$

due to the facts that $\lim_{L\to 0+} T(E,L) = A(E)$ and $T(E,L)$ is monotone for L on the small interval $[0, a_1]$. We numerically compute the coefficient on the right side of (14) by choosing $a_1 = 0.01$, then

$$\frac{64}{6}\pi^3 \int_4^5 |\mu'(E)| \max\left\{A(E), T(E, a_1)\right\} dE = 3.787856674901141 \times 10^2.$$

Thus $a_1 = 0.01$ is enough to make the first error to be of order 10^{-10}.

The error on $[L_{max} - a_2, L_{max}]$ is

$$\left| 32\pi^3 \int_4^5 \int_{L_{max}-a_2}^{L_{max}} \mu'(E)\, L^4 \int_{r_1(E,L)}^{r_2(E,L)} (\phi - \overline{\phi})^2 \frac{2L dr dL dE}{\sqrt{2(E - U(r) - L^2/2r^2)}} \right| \tag{15}$$
$$\leq 64\pi^3 \int_4^5 L_{max}(E)^5 |\mu'(E)| \max\left\{ \frac{\pi}{\sqrt{\phi''_{\text{eff}}(r^*; L_{\max})}}, T(E, L_{\max} - a_2) \right\} dE\ a_2.$$

where the effective potential

$$\phi_{\text{eff}}(r) = U_0(r) + L^2/2r^2$$

Since

$$T(E,L) \leq \max\left\{ \frac{\pi}{\sqrt{\phi''_{\text{eff}}(r^*; L_{\max})}}, T(E, L_{\max} - a_2) \right\},\ L \in [L_{\max} - a_2, L_{\max}],$$

due to the facts that $\lim_{L\to L_{\max}-} T(E,L) = \frac{\pi}{\sqrt{\phi''_{\text{eff}}(r^*; L_{\max})}}$ and $T(E,L)$ is monotone for L on $[L_{\max} - a_2, L_{\max}]$.

Numerically computing the coefficient before a_2 in the right hand side of (15), we get 0.605275913474830. Choose $a_2 = 10^{-5}$, the right side of (15) if of order 10^{-5}, which is good enough for what we need later on.

Step 5. Conclusion. We choose $\phi(r) = e^{-r}$. The first term of (6) is $\int |\nabla\phi|^2 = \pi$, and the second term is computed to be -31.733535998660550, by choosing $h = 0.1$ in Runga-Kutta Method when solving $U(r)$. Therefore $(A\phi, \phi) = \pi - 31.733535998660550 < 0$. We gradually decrease h, and repeat the whole process to calculate the second term of (6). The result is shown in Table 4. Thus when h becomes smaller, the second term of (6) is less than -45. Combining with the error estimates of (14) and (15) in Step 4, we can ensure $(A_0\phi, \phi) < 0$.

TABLE 4. results for different h

h	the second term
0.1	-31.733535998660550
0.05	-38.227746546049751
0.025	-41.848643231095494
0.01	-44.146480909452201
0.005	-44.933896897054382
0.0025	-45.331673900274509
0.001	-45.571655158578380

3.2. **Numerical Computation for Example 2.** With profile (9), we choose $\phi(r)$ to be a linear combination of several functions $e^{-\alpha_i r},\ 1 \le i \le n,\ \phi(r) = \sum a_i e^{-\alpha_i r}$, with a_i to be determined. In the quadratic form (6), the first term is computed to be

$$\int |\nabla\phi|^2 = 4\pi(\sum \frac{a_i^2}{4\alpha_i} + \sum \frac{4\alpha_i\alpha_j}{(\alpha_i+\alpha_j)^3} a_i a_j) \triangleq \sum b_i a_i^2 + 2\sum b_{ij} a_i a_j$$

and the second term is

$$\begin{aligned}
&32\pi^3 \int f_0'(E,L) \int_{r1(E,L)}^{r2(E,L)} (\sum a_i\phi_i - \overline{\sum a_i\phi_i})^2 \frac{2LdrdEdL}{\sqrt{2(E-U_0(r)-L^2/2r^2)}} \\
&= \sum 32\pi^3 \int f_0'(E,L) \int_{r1(E,L)}^{r2(E,L)} (\phi_i - \overline{\phi_i})^2 \frac{2LdrdEdL}{\sqrt{2(E-U_0(r)-L^2/2r^2)}} a_i^2 + \\
&\sum 32\pi^3 \int f_0'(E,L) \int_{r1(E,L)}^{r2(E,L)} (\phi_i - \overline{\phi_i})(\phi_j - \overline{\phi_j}) \frac{2LdrdEdL}{\sqrt{2(E-U_0(r)-L^2/2r^2)}} 2a_i a_j \\
&\triangleq \sum c_i a_i^2 + \sum 2c_{ij} a_i a_j
\end{aligned}$$

Now $(A_0\phi,\phi) = \sum(b_i+c_i)a_i^2 + 2\sum(b_{ij}+c_{ij})a_i a_j$. The corresponding matrix for this quadratic form is $S = (s_{ij})$, where $s_{ii} = b_i + c_i, \quad s_{ij} = b_{ij} + c_{ij}$. Denote $\lambda_{\min}$ to be the minimum eigenvalue of the matrix S, then $\lambda_{\min} < 0$ guarantees that there exists ϕ such that $(A_0\phi,\phi) < 0$. We choose

$$\phi_1 = e^{-r},\ \phi_2 = e^{-\frac{1}{2}r},\ \phi_3 = e^{-\frac{1}{3}r},\ \phi_4 = e^{-2r},\ \phi_5 = e^{-3r},\ \phi_6 = e^{-4r},\ \phi_7 = e^{-5r}.$$

In (9), there are five free parameters in μ: a, k, t_1, E_0, C_1 and E_1 is determined by $E_1 = (E_0 + t_1 a)/(t_1+1)$. Using U_0 (the initial value of the potential) as an additional parameter, there are totally six parameters in our calculations. The idea is to view λ_{min} as a function of these parameters $\lambda_{min} = \lambda_{min}(a, k, t_1, E_0, C_1, U_0)$. Our goal now is to find proper parameters such that $\lambda_{min} < 0$. The numerical methods are the same as in *Step 1-Step 3* in the computation of Example 1, except that now we use self-adaptive Runge-Kutta Method to solve (11). We next verify that the following choice of parameters

$$C_1 = 2,\ E_0 = 5.1,\ a = 1.9,\ k = 2.01,\ t_1 = 1.5,\ U_0 = -15.1,$$

would lead to $\lambda_{min} < 0$ and $(A_0\phi,\phi) < 0$. In Table 5 we show the results of $\lambda_{\min}$ under different accuracies. where a_1 and a_2 are the parameters used to truncate $[0, L_{\max}]$ to $[a_1, L_{\max} - a_2]$. We also calculate the eigenvector corresponding to

TABLE 5. λ_{min} under different accuracies

integration accuracy	a_1	a_2	accuracy of the roots	λ_{min}
10^{-8}	10^{-5}	10^{-6}	10^{-10}	$-1.808068979998836 \times 10^{-5}$
10^{-9}	10^{-3}	10^{-4}	10^{-10}	$-3.403231868973289 \times 10^{-6}$
10^{-9}	10^{-5}	10^{-6}	10^{-11}	$-3.739973399333609 \times 10^{-6}$
10^{-10}	10^{-5}	10^{-6}	10^{-11}	$-3.196606813186484 \times 10^{-6}$
10^{-11}	10^{-5}	10^{-6}	10^{-11}	$-3.025099283901562 \times 10^{-6}$
10^{-12}	10^{-6}	10^{-7}	10^{-11}	$-3.087487453314562 \times 10^{-6}$
10^{-13}	10^{-6}	10^{-7}	10^{-11}	$-3.080483943121587 \times 10^{-6}$
10^{-13}	10^{-6}	10^{-7}	10^{-11}	$-3.089704058599446 \times 10^{-6}$
10^{-14}	10^{-7}	10^{-7}	10^{-11}	$-3.089187445892979 \times 10^{-6}$

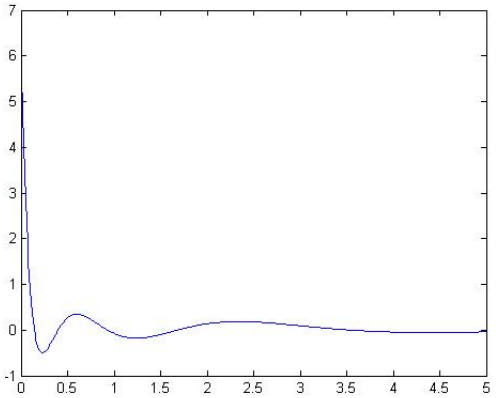

FIGURE 10. $\phi(r)$

$\lambda_{\min}$ by $v = (v_1, v_2, v_3, v_4, v_5, v_6, v_7)^T$, where

$$\begin{aligned} v_1 &= 41.702767064740 \\ v_2 &= -14.949618378683 \\ v_3 &= 4.856846351504 \\ v_4 &= -201.361293458803 \\ v_5 &= 571.694416252419 \\ v_6 &= -723.292461038838 \\ v_7 &= 327.842857021134. \end{aligned} \tag{16}$$

Let

$$\phi(r) = v_1 e^{-r} + v_2 e^{-\frac{1}{2}r} + v_3 e^{-\frac{1}{3}r} + v_4 e^{-2r} + v_5 e^{-3r} + v_6 e^{-4r} + v_7 e^{-5r}.$$

We draw a picture of this function ϕ in Figure 10. Using (6), we obtain

$$(A\phi, \phi) = 35.231484866282720 - 59.247837621248109 < 0,$$

when the integration accuracy is 10^{-13}, $a_1 = 10^{-6}$, $a_2 = 10^{-7}$, and the root accuracy is 10^{-11}.

Step 4. Error Estimate. We obtain theoretical error estimate as in Example 1. For any test function ϕ, the error for L on $[0, a_1]$ is

$$\left|32\pi^3 \int_{\{E|\mu'(E)>0\}} \mu'(E) \int_0^{a_1} \int_{r_1(E,L)}^{r_2(E,L)} (\phi - \overline{\phi})^2 \frac{2LdrdLdE}{\sqrt{2(E - U_0 - L^2/2r^2)}}\right|$$
$$\leq 32\pi^3 |\max\phi - \min\phi|^2 a_1^2 \int_{\{E|\mu'(E)>0\}} \mu'(E) \max\{A(E), T(E, a_1)\} dE$$

Numerically compute the right hand side, and note

$$|\max\phi - \min\phi| \leq 2\max|\phi| \leq 2\sum|v_i| = 3.7714 \times 10^3.$$

Choose $a_1 = 10^{-5}$, the error is no more than

$$4.322 \times 10^2 \times (3.7714 \times 10^3)^2 \times (10^{-5})^2 = 6.1474 \times 10^{-1}$$

Next we estimate the error for L on $[L_{\max} - a_2, L_{\max}]$. When $r \in [r_1, r_2]$, we use $|\phi - \overline{\phi}| \leq \max|\phi'|(r_2 - r_1)$ by the Mean Value Theorem. So the error is

$$32\pi^3 \int_{\{E|\mu'(E)>0\}} \int_{L_{max}-a_2}^{L_{max}} \int_{r_1(E,L)}^{r_2(E,L)} \mu'(E)(\phi - \overline{\phi})^2 \frac{2LdrdLdE}{\sqrt{2(E - U_0 - L^2/2r^2)}}$$
$$\leq 64\pi^3 a_2 |\phi'|_{L^\infty}^2 \int_{\{E|\ \mu'(E)>0\}} \mu'(E) L_{\max}(E) \left(r_2(E, L_{\max} - a_2) - r_1(E, L_{\max} - a_2)\right)^2 \cdot$$
$$\max\left\{\frac{\pi}{\sqrt{\phi''_{\text{eff}}(r^*; L_{\max})}}, T(E, L_{\max} - a_2)\right\} dE\ .$$

Note that

$$\max\ |\phi'| \leq 5\sum|v_i| = 9.4285 \times 10^3.$$

Numerically computation of this error with $a_2 = 10^{-7}$ yields a bound of

$$1.41722 \times 10^{-13} \times (9.4285 \times 10^3)^2 = 1.3362 \times 10^{-6}$$

So the total error is at most of order 10^{-1}, which guarantees $(A\phi, \phi) < 0$.

4. **Summary**

We study the instability of spherical galaxy models in the Vlasov theory for collisionless stars. Based on the instability criterion of Theorem 1 and careful numerical computations, we have constructed two explicit *unstable* galaxy models $f_0(E, L)$ and $f_0(E)$ with distributions (8) and (9) respectively. In particular, $f_0(E)$ in Example 2 provides the first example of unstable isotropic galaxy which has not been found in literature. The instability in these examples are radial and non-oscillatory. Compared with the usual N-body codes of finding instability of galaxy models, our method only requires numerical evaluation of certain explicit integrals. Therefore, it is much more reliable and easier to implement. It is hoped that Theorem 1 can be employed to detest instability for other galaxy models in the future.

Acknowledgements

This research is supported partly by NSF grants DMS-0603815 and DMS-0505460 (Guo) and DMS-0908175 (Lin). We would like to dedicate this paper to the memory of Seiji Ukai.

References

[1] V. A. Antonov, *Remarks on the problem of stability in stellar dynamics.* Soviet Astr. J., **4** (1961) 859-867.

[2] V. A. Antonov, *Solution of the problem of stability of stellar system Emden's density law and the spherical distribution of velocities*, Vestnik Leningradskogo Universiteta, Leningrad University, 1962.

[3] J. Barnes; P. Hut; J. Goodman, Dynamical instabilities in spherical stellar systems, Astrophysical Journal, **300** (1986), 112-131.

[4] P. Bartholomew, *On the theory of stability of galaxies*, Monthly Notices of the Royal Astronomical Society, **151** (1971), 333-350.

[5] G. Bertin, Dynamics of Galaxies, Cambridge University Press, 2000.

[6] J. Binney and S. Tremaine, *Galactic Dynamics (2nd edition).* Princeton University Press, 2008.

[7] J. P. Doremus; M. R. Feix; G. Baumann, *Stability of Encounterless Spherical Stellar Systems*, Phys. Rev. Letts, **26** (1971), 725-728.

[8] D. Gillon; M. Cantus; J. P. Doremus; G. Baumann, *Stability of self-gravitating spherical systems in which phase space density is a function of energy and angular momentum, for spherical perturbations*, Astronomy and Astrophysics, **50** (1976), 467-470.

[9] A. Fridman and V. Polyachenko, *Physics of Gravitating System Vol I,* Springer-Verlag, 1984.

[10] J. Goodman, *An instability test for nonrotating galaxies*, Astrophysical Journal, **329** (1988), 612-617.

[11] Y. Guo and Z. Lin, *Unstable and stable galaxy models.* Commun. Math. Phys., **279** (2008), 789–813.

[12] M. Henon, *Numerical Experiments on the Stability of Spherical Stellar Systems*, Astronomy and Astrophysics, **24** (1973), 229-238.

[13] Y. Guo and G. Rein, *A non-variational approach to nonlinear stability in stellar dynamics applied to the King model*, Comm. Math. Phys., **271** (2007), 489-509.

[14] H. Kandrup and J. F. Signet, *A simple proof of dynamical stability for a class of spherical clusters.* The Astrophys. J. **298** (1985), 27-33.

[15] H. Kandrup, *A stability criterion for any collisionless stellar equilibrium and some concrete applications thereof*, Astrophysical Journal, **370** (1991), 312-317.

[16] D. Merritt, *Elliptical Galaxy Dynamics*, The Publications of the Astronomical Society of the Pacific, **111** (1999), Issue 756, 129-168.

[17] P. L. Palmer, *Stability of collisionless stellar systems: mechanisms for the dynamical structure of galaxies*, Kluwer Academic Publishers, 1994.

[18] J. Perez and J. Aly, *Stability of spherical stellar systems - I. Analytical results*, Monthly Notices of the Royal Astronomical Society, **280** (1996), 689-699.

[19] J. F.Sygnet; G. des Forets; M. Lachieze-Rey; R. Pellat, *Stability of gravitational systems and gravothermal catastrophe in astrophysics*, Astrophysical Journal, **276** (1984), 737-745.

[20] G. Rein and A. D. Rendall, *Compact support of spherically symmetric equilibria in non-relativistic and relativistic galactic dynamics,* Math. Proc. Camb. Phil. Soc. **128** (2000), 363-380.

School of Mathematical Sciences, Peking University, Beijing, 100871, P. R. China

Division of Applied Mathematics, Brown University, Providence, RI 02912, USA

School of Mathematics, Georgia Institute of Technology, Atlanta, GA 30332, USA

School of Mathematical Sciences, Peking University, Beijing, 100871, P. R. China